

# The Newton variational functional for the log-derivative matrix: Use of the reference energy Green's function in an exchange problem

B. Ramachandran

Department of Chemistry, Louisiana Tech University, Ruston, Louisiana 71272

Michael D'Mello and Robert E. Wyatt

Department of Chemistry and Biochemistry and The Institute for Theoretical Chemistry, University of Texas, Austin, Texas 78712

(Received 6 July 1990; accepted 17 August 1990)

The Newton Variational Principle for the log-derivative matrix (the Y-NVP) is studied in the context of a collinear exchange problem. In contrast to the integral equation methods that calculate the  $K$  or the  $T$  matrices directly, the matrix elements of the log-derivative Newton functional can be made independent of the scattering energy. This promises considerable savings in computational effort when state to state transition probabilities are calculated at several energies, since the matrix elements of the functional need be calculated only once. Green's functions defined with respect to a reference energy, called the reference energy Green's functions (or the REGFs), play a central role in the Y-NVP functional. The REGFs may be defined with or without reference to asymptotic channel energies. If channel dependent REGFs are used, the Y-NVP converges at the same rate as the GNVP for the  $K$  or  $T$  matrices, when the scattering energy is the same as the reference energy. On the other hand, channel independent REGFs permit even further reductions in computational effort. We use both types of REGFs in the present paper, and compare the rates of convergence. These comparisons show that the convergence rate of the method is *not significantly altered by the type of REGF used*. Further, we show that the Y-NVP is able to achieve rapid convergence of reactive transition probabilities over a large range of scattering energies, even when scattering resonances are present. An analysis of the computational effort required for each part of the calculation leads to the conclusion that a Y-NVP calculation using a channel independent REGF requires *essentially only the same amount of computer time as a log-derivative Kohn (Y-KVP) calculation, while, presumably, offering faster convergence*.

## I. INTRODUCTION

The last few years have witnessed exciting developments in the theoretical study of chemical reaction dynamics. The result of these recent developments has been that several independent, well-converged calculations of integral and differential cross sections have been completed for the  $H + H_2$  reaction.<sup>1-5</sup> The methods used for these calculations may be broadly classified into two categories:  $L^2$  variational methods utilizing Jacobi coordinates in each arrangement channel,<sup>1-4</sup> and those that resort to solution propagation in hyperspherical coordinates.<sup>5</sup> In addition to these calculations, accurate 3D reactive transition probabilities for the  $H + H_2$  reaction have also been computed by methods developed by the research groups of Pack,<sup>6</sup> Kuppermann,<sup>7</sup> Schatz,<sup>8</sup> Baer,<sup>9</sup> Light<sup>10</sup> and Lindeberg *et al.*<sup>11</sup> It should be noted that any of these approaches are capable of generating integral and differential cross sections for this reaction.

Variational methods that have been used in recent years in various scattering calculations can be further classified into two categories: one, those derived directly from the Schrödinger (differential) equation, such as the  $S$ -matrix Kohn method (the S-KVP),<sup>1,2,12-14</sup> or the log-derivative Kohn method (the Y-KVP);<sup>3,15,16</sup> and two, those derived from the Lippmann-Schwinger (integral) equation, such as

the Schwinger variational principle (SVP),<sup>17</sup> the  $L^2$  amplitude density generalized Newton variational principle ( $L^2$  AD-GNVP),<sup>17-20</sup> and the log-derivative Schwinger (Y-SVP) and Newton (Y-NVP) methods.<sup>21</sup> The Y-NVP functionals for potential and inelastic scattering were derived and applied to a few model problems in Ref. 21. The present work derives the Y-NVP functional for reactive scattering, where the amplitude density is expanded in an  $L^2$  basis set. Several issues concerning the application of the method are investigated using the simplest case of reactive scattering, viz., the collinear  $H + H_2$  problem, as an example.

The main features of the Y-NVP are the following. In contrast to the integral equation methods that calculate the  $K$  or the  $T$  matrices directly (such as the GNVP), the matrix elements of the Y-NVP functional can be made independent of the scattering energy. Green's functions defined with respect to a reference energy, called the *reference energy Green's functions* (or the REGFs), play the same role in the Y-NVP functional as those defined with respect to asymptotic channel translational energies in the GNVP. The REGFs may be defined with or without reference to internal energies. If channel dependent REGFs are used, the Y-NVP converges at the same rate as the GNVP for the  $K$  or  $T$  matrices, when the scattering energy is the same as the reference energy. On the other hand, channel independent REGFs permit even further reductions in computational effort.

These features of the Y-NVP must be considered in the context of the two main areas where computational effort is expended in applying  $L^2$  variational methods: one, the evaluation of matrix elements of the variational functional, and two, the solution of a (usually large) system of linear algebraic equations. The consensus is that if the linear system is large enough, the latter step will dominate the calculation. This being the case, integral equation methods, particularly the GNVP, seem superior to the Kohn methods, since previous comparisons<sup>22-24</sup> show that the GNVP converges with fewer basis functions than the Kohn methods.

However, the computational effort to evaluate the matrix elements of the Kohn and Newton functionals is not the same. The Kohn functional is very simple, and the only elements needed are those of the Hamiltonian and the overlap matrices. The two Kohn methods also have the advantage that all or almost all matrix elements of the functional are energy independent. This means that the first part of the calculation need be performed only once. The GNVP functional on the other hand, is quite a bit more complex, and contains integral operators involving the Green's function for a reference problem. For most choices of the reference problem, the Green's functions have to be numerically evaluated before the calculation of matrix elements can begin. Also, the scattering energies are deeply embedded in the GNVP functional through the Green's functions. This makes it necessary to evaluate the Green's functions and the matrix elements of the functional at each scattering energy. The second part of the calculation, i.e., solving the linear system of equations, remains explicitly energy dependent in either approach.

Many of the interesting features of scattering events, such as scattering resonances, become evident only when transition probabilities are calculated at a number of energies. Therefore, methods for reactive scattering should strive to minimize computational time required per energy. This would mean that the system of linear equations be as small as possible—which suggests a rapidly convergent integral equation method such as the GNVP—and the effort expended in matrix element evaluation at each energy be minimal—which suggests a method in which the matrix elements are energy independent, such as the Kohn methods. The topic of the present paper, viz., the Y-NVP, combines these seemingly irreconcilable features, and is, therefore, a method that shows much promise for future applications.

The present implementation of the Y-NVP differs from that of Ref. 21 in two important ways. One, the basis set used to expand the amplitude densities now includes a function that satisfies the log-derivative boundary conditions. While the method still achieves rapid convergence in the absence of this function for energies fairly close to the reference energy (for reasons to be explained in Sec. II D), its presence significantly increases the range of energies over which the REGFs are effective. Two, as a result of this addition to this basis, we find that it is no longer necessary to define the REGFs with reference to the asymptotic channel energies, as done in Ref. 21. This has important consequences, one of which is that it is now possible to perform a Y-NVP calculation *using essentially only the same amount of computer time*

*required for a Y-KVP calculation.* These ideas are illustrated using the collinear H + H<sub>2</sub> system on the PK2 potential surface<sup>25</sup> as an example. A number of exact quantum mechanical results are available for this system.<sup>26,27</sup> The energy range we examine contains a number of scattering resonances, and the number of open channels increase from one at the bottom of the range to three near the top.

The remainder of this paper is organized as follows: in Sec. II, we present the theory of the log-derivative Newton method as applied to a multi-arrangement scattering problem. Our formulation is based on Miller's approach to reactive scattering<sup>28</sup> which has been used by many workers.<sup>1-4,13-20,26</sup> Section III describes the details of our numerical calculations, and presents the results. Section IV summarizes the present work and presents typical CPU times for the Y-NVP calculations. Two Appendices are presented at the end of the paper. Appendix A establishes the explicit mathematical relationships between the Kohn, Schwinger and Newton variational functionals for the log-derivative. Appendix B discusses a topic of considerable importance: the possibility of encountering anomalous singularities in the Y-NVP.

## II. THE LOG-DERIVATIVE NEWTON METHOD FOR REACTIVE SCATTERING

### A. Boundary conditions and the reference energy Green's functions

Consider the one-dimensional problem

$$\left[ \frac{-d^2}{dR^2} + U(R) - k^2 \right] \varphi(R) = 0, \quad (1)$$

where  $U(R) = 2\mu V(R)/\hbar^2$  and  $k^2 = 2\mu E/\hbar^2$ . It is easy to show, by requiring that  $\varphi(0) = 0$ , that the log-derivative  $Y(a) = \varphi'(R)/\varphi(R)|_{R=a}$  satisfies

$$\int_0^a dR (d\varphi/dR)^2 + \int_0^a dR \varphi(R) \times [U(R) - k^2] \varphi(R) = Y(a)\varphi(a)^2. \quad (2)$$

This of course, is a result from Kohn's celebrated paper of 1948.<sup>29</sup> By requiring that  $\varphi(a) = 1$ , Eq. (2) can be made to directly yield the log-derivative at  $R = a$ —a fact utilized by Manolopoulos and Wyatt.<sup>15</sup> The boundary conditions imposed on the solution are thus,  $\varphi(0) = 0$  and  $\varphi(a) = 1$ . We refer to these as the log-derivative or the "(0,1)" boundary conditions. Following this convention, below, we also refer to functions that satisfy the (0,0) or the (1,0) boundary conditions in the interval (0,a).

Let us consider the reference problem

$$\left[ \frac{-d^2}{dR^2} + U_D(R) - \kappa^2 \right] \varphi(R) = 0; \quad 0 \leq R \leq a, \quad (3)$$

where  $U_D(R) = 2\mu V_D(R)/\hbar^2$  is a distortion potential, and  $\kappa^2 = 2\mu E_{\text{ref}}/\hbar^2$ , where  $E_{\text{ref}}$  is the reference energy. The solution  $\varphi(R)$  satisfies the (0,1) or the (1,0) boundary conditions depending on whether we solve for the regular or irregular solution, respectively. The Newton variational functional requires the Green's function as well as the regular solution to the reference problem. Below, we outline a

method by which these may be generated in a *variational* manner.

The distorted wave Green's function for the reference problem of Eq. (3) satisfies

$$\left[ \frac{-d^2}{dR^2} + U_D(R) - \kappa^2 \right] G^D(R, R') = -2\mu\delta(R - R')/\hbar^2. \quad (4)$$

It follows from the work of Miller and Jansen op de Haar<sup>12</sup> that a variational expression for this Green's function would be

$$G^D(R, R') = \sum_{i,j=1}^{N-1} \langle R | u_i \rangle \left[ \langle u_i | \kappa^2 + \frac{d^2}{dR^2} - U_D(R) | u_j \rangle^{-1} \right] \langle u_j | R' \rangle, \quad (5)$$

where the  $L^2$  basis set  $\{u_i\}_1^N$  is such that  $u_i(0) = u_i(a) = 0$  for  $i < N$ ,  $u_N(0) = 0$  and  $u_N(a) = 1$ . [It is important to note in Eq. (5) [as well as in Eqs. (16) and (36) below], that the quantity enclosed in square brackets is the  $(ij)$ th element of the matrix inverse, rather than the inverse of the  $(ij)$ th element. This notation,<sup>12</sup> while lacking in rigor, has the advantage of showing the composition of the matrix that is inverted in an explicit and compact manner.] The restriction of the basis functions in Eq. (5) to the subset  $\{u_i\}_1^{N-1}$  is due to the fact that the kernel of the Green's function vanishes at both ends of the interval  $(0, a)$ .<sup>30</sup> The function  $u_N$  serves to enforce the  $(0,1)$  boundary conditions in the regular solution.

Expanding  $\varphi(R)$  in the basis  $\{u_i\}_1^N$ , the reference problem of Eq. (3) is written as

$$\sum_{j=1}^N \left[ \frac{-d^2}{dR^2} + U_D(R) - \kappa^2 \right] u_j(R) C_j = 0 \quad 0 \leq R \leq a. \quad (6)$$

Since all basis functions except  $u_N$  vanish at  $R = a$ , and since both the solution  $\varphi(R)$  and  $u_N(R)$  satisfy the same boundary condition at  $R = a$ , it is obvious that  $\varphi(a) = u_N(a)$ . Therefore,  $C_N = 1$ . We now rearrange Eq. (6) to give

$$\sum_{j=1}^{N-1} \{ -u_j'' + [U_D(R) - \kappa^2] u_j \} C_j = u_N'' - [U_D(R) - \kappa^2] u_N. \quad (7)$$

Premultiplying both sides with basis functions  $u_i$ , and integrating, we get

$$\sum_{j=1}^{N-1} \left[ \int_0^a (u_i' u_j') dR + \int_0^a u_i (U_D - \kappa^2) u_j dR \right] C_j = \int_0^a (u_i' u_N') dR - \int_0^a u_i (U_D - \kappa^2) u_N dR \quad i = 1, \dots, N-1. \quad (8)$$

The surface terms on the right-hand side of Eq. (8),  $-u_i u_N' |_{R=0}^R = 0$  vanish because of the  $(0,0)$  boundary conditions imposed on the  $u_i(R)$  for  $i < N$ . The linear algebraic problem of Eq. (8), of the type  $\mathbf{AC} = \mathbf{b}$  can now be solved for the unknown coefficients  $\mathbf{C}$  as  $\mathbf{A}^{-1}\mathbf{b}$ . Inserting  $-\mathbf{A}^{-1}$  into

Eq. (5) yields the kernel of the Green's function, while the regular solution  $\varphi(R)$  is given by

$$\varphi(R) = u_N(R) + \sum_{i=1}^{N-1} u_i(R) C_i. \quad (9)$$

Note that the irregular solution, which satisfies the  $(1,0)$  boundary conditions in  $(0, a)$  can also be easily generated by the above treatment, the only change being the addition of a function  $u_0(R)$ , which satisfies the  $(1,0)$  boundary conditions, to the basis. This results in a second right-hand side to Eq. (8), whose solution yields the desired function.

The fact that a matrix inversion (which scales as  $N^3$  for a direct method) is required to evaluate the Green's function, is certainly a disadvantage of this approach. However, note that Eq. (5) is a *variational* expression, and therefore, promises to yield highly accurate solutions for relatively modest basis sizes. Nevertheless, in a multichannel problem, if the distortion potential  $U_D$  couples several channels, the order of this matrix will be quite large. With this in mind, we are at present, exploring different ways of calculating distorted wave Green's functions in an efficient manner.<sup>31</sup>

To evaluate the Green's functions for the collinear  $H + H_2$  problem, we proceed as follows. For the basis set  $\{u_i\}_1^N$ , we choose an  $N$  member Lagrange polynomial set defined over the nodes of an  $(N+1)$  point Gauss-Lobatto quadrature rule, in an interval  $(R_{\min}, R_{\max}) = (R_0, R_N)$ . The function  $u_0(R)$  that goes to unity at  $R_0$  is not included in the basis. At the quadrature points, the basis satisfies  $u_i(R_j) = \delta_{ij}$ , where the quadrature points are labeled in the increasing order from 0 corresponding to  $R_0$ , to  $N$  corresponding to  $R_N$ . This results in a discrete variable representation (DVR) of the reference problem, identical to the one employed by Manolopoulos and Wyatt in their first application of the Y-KVP.<sup>15</sup> The following simplification can be made immediately: since in the Lobatto DVR, the functions  $\{u_i\}$  form an orthogonal set, the potential  $U_D$  is diagonal in this representation. Therefore, the only integrals that require summation over the quadrature nodes are those involving the derivatives of the basis functions.

In the discrete variable representation, the Green's function at a point  $(R, R') = (R_i, R_j)$  is given by

$$G^D(R_i, R_j) = -(\mathbf{A}^{-1})_{ij} \quad i, j = 1, \dots, N-1.$$

Since  $G^D(R_0, R) = G^D(R, R_0) = G^D(R_N, R) = G^D(R, R_N) = 0$ ,<sup>30</sup> this completely defines the Green's functions. The regular solution to the reference problem, recognizing the orthonormal nature of the basis in the DVR, is given by

$$\varphi(R_j) = \delta_{Nj} + C_j(1 - \delta_{Nj}) \quad j = 1, \dots, N.$$

The accuracy of this treatment can be illustrated by computing the free wave Green's functions  $G^0(R, R')$  for the special case of the hard sphere distortion potential:  $U_D(0) = \infty, U_D(R) = 0$  elsewhere. In this case, the reference problem can be solved analytically<sup>21</sup> and the results are

$$G^0(R, R') = \begin{cases} -\{\sin(\kappa R_<) \sin[\kappa(a - R_>)]\} [\kappa \sin(\kappa a)]^{-1} & \kappa^2 > 0 \\ -\{\sinh(\kappa R_<) \sinh[\kappa(a - R_>)]\} [\kappa \sinh(\kappa a)]^{-1} & \kappa^2 < 0 \end{cases} \quad (10)$$

where  $(R_-, R_+)$  are the lesser and greater, respectively, of  $(R, R')$ . The results of computing  $G^0(R, R')$  using Eq. (5) is shown in Fig. 1 for a certain value of  $R'$ . It is clear that the variational expression of Eq. (5) is very accurate everywhere, except for the small differences at the "kink" in the Green's functions, at  $R = R'$ . These errors can of course, be made smaller by choosing a larger basis (i.e., a finer grid) to represent the Green's function. However, our convergence checks show that the present grid is sufficient to satisfactorily converge the matrix elements of the functional.

## B. The Y-NVP functional for reactive scattering

Derivations of the Y-NVP functional for potential and inelastic scattering are given in Ref. 21. A derivation starting from Kohn's variational functional for the  $Y$  matrix<sup>15,16,29</sup> is also provided in Appendix A of the present paper. The treatment below explicitly considers the case of reactive scattering.

forms the basis for Miller's exchange formalism.<sup>28</sup>

As in any quantum mechanical problem, our aim is to find solutions to the problem

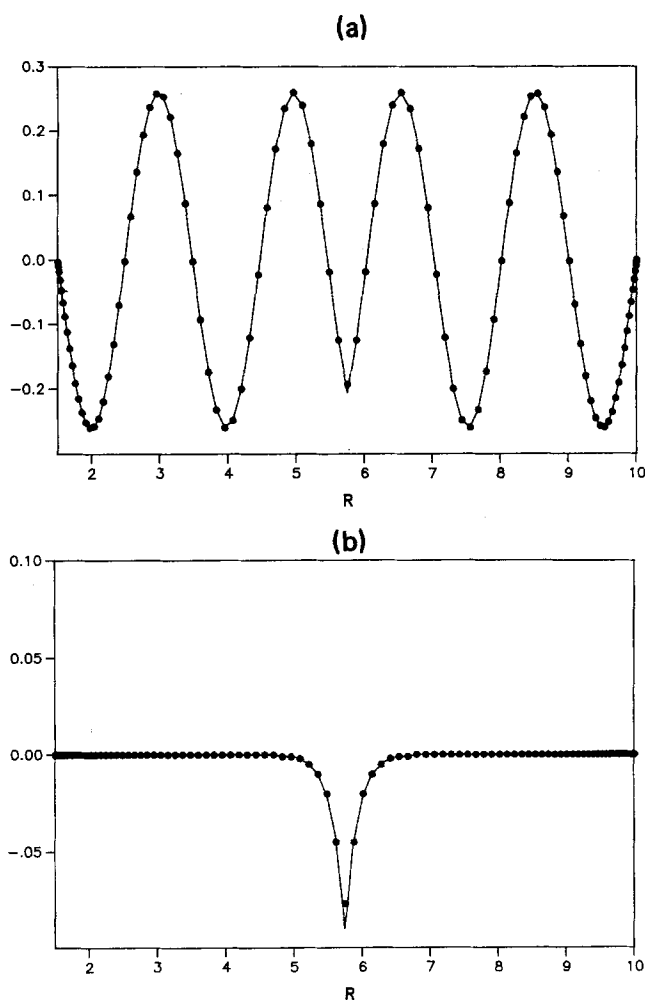


FIG. 1. Reference energy Green's functions. The circles represent the variational expression of Eq. (5) at the nodes of a 101 point Gauss-Lobatto quadrature rule, whereas the curve represents the analytic solutions of Eq. (10). (a) An open channel Green's function. (b) A closed channel Green's function.

$$(H - E)\Psi = 0. \quad (11)$$

We begin by writing the Hamiltonian in arrangement  $\alpha$  as

$$H_\alpha(R_\alpha, r_\alpha) - E = T_\alpha(R_\alpha, r_\alpha) + h_\alpha(r_\alpha) + V_\alpha(R_\alpha, r_\alpha) - E, \quad (12)$$

where the first three terms on the right-hand side are, respectively, the kinetic, internal and potential terms,  $E$  is the scattering energy and the coordinates  $(R_\alpha, r_\alpha)$  are the mass-weighted, isoinertial<sup>32</sup> Jacobi coordinates commonly used in reactive scattering. We expand the wave function for scattering initiated in, say, the internal state  $n$  of arrangement  $\alpha$ , in terms of all the internal states and all the arrangements:

$$\Psi_{\alpha n} = \sum_{\beta m} \psi_{\alpha n}^{\beta m} = \sum_{\beta m} \phi_{\beta m}(r_\beta) f_{\alpha n}^{\beta m}(R_\beta), \quad (13)$$

where the  $\phi_{\beta m}$  satisfy  $h_\beta \phi_{\beta m} = \epsilon_{\beta m} \phi_{\beta m}$ . This type of expansion for the scattering wave function has also been called the Fock coupling scheme,<sup>17</sup> because it is similar in spirit to the Hartree-Fock method for electronic structure calculations. [A few comments about the notation are in order. We use Greek superscripts and subscripts to denote arrangements, and lower case *italic* letters for internal state labels. For compactness of notation, the quantity  $f_{\beta m \rightarrow \alpha n}(R_\beta)$  is written above as  $f_{\alpha n}^{\beta m}(R_\beta)$ . We use the same convention for all functions and matrix elements. So, for example,  $Z_{\alpha n, \beta m}$  (see below) is written as  $Z_{\beta m}^{\alpha n}$ , i.e., the row index is the superscript, and the column index is the subscript.]

The next step is to identify the reference problem for the Green's functions. As mentioned in Sec. I, the reference energy Green's functions (the REGFs) for the Y-NVP may be defined with or without reference to the asymptotic internal energies. In this section, we derive our equations using a set of channel dependent REGFs. In Sec. II C, we discuss the channel independent REGFs and the advantages that they promise. Thus, we now define the reference problem in arrangement  $\alpha$  as

$$[T_\alpha(R_\alpha, r_\alpha) + h_\alpha(r_\alpha) - E_{\text{ref}}] f_{\alpha n}^0(R_\alpha) \phi_{\alpha n}(r_\alpha) = 0, \quad (14)$$

where  $E_{\text{ref}}$  is a reference energy (a constant, as far as this development is concerned). The functions  $f_{\alpha n}^0(R_\alpha)$  satisfy the (0,1) boundary conditions. Note that the distortion potential used is that of the hard sphere problem. For later use, we identify the remainder of the full problem, i.e., the part of Eq. (12) that was excluded from the reference problem of Eq. (14), as

$$Z_\alpha(R_\alpha, r_\alpha) = U_\alpha(R_\alpha, r_\alpha) - \lambda, \quad (15)$$

where

$$U_\alpha(R_\alpha, r_\alpha) = 2\mu V_\alpha(R_\alpha, r_\alpha) / \hbar^2$$

and

$$\lambda = 2\mu(E - E_{\text{ref}}) / \hbar^2 = k^2 - \kappa^2.$$

The reference energy Green's functions  $G_{\alpha n}^0(R_\alpha, r_\alpha; R'_\alpha, r'_\alpha)$  are now calculated as<sup>33</sup>

$$\begin{aligned} \mathbf{G}_{\alpha n}^0 &= \sum_{ij} |u_i \phi_{\alpha n}\rangle \\ &\times (\langle \phi_{\alpha n} u_j | \kappa^2 - h_{\alpha} - T_{\alpha} | u_j \phi_{\alpha n}\rangle^{-1}) \langle \phi_{\alpha n} u_j | \\ &= |\phi_{\alpha n}\rangle \mathbf{G}_{\alpha n}^0 \langle \phi_{\alpha n}|, \end{aligned} \quad (16)$$

where the functions  $\{u_i\}$  are the same as those described in Sec. II A.

We now define the projected amplitude densities<sup>17</sup> as

$$F_{\beta m}^{\alpha n}(\mathbf{R}_{\alpha}) = \sum_{\gamma l} \mathbf{Z}_{\gamma l}^{\alpha n} f_{\beta m}^{\gamma l}(\mathbf{R}_{\gamma}),$$

where if  $\alpha = \gamma$ ,  $\mathbf{Z}_{\gamma l}^{\alpha n}$  is the direct interaction potential

$$\mathbf{Z}_{\alpha l}^{\alpha n}(\mathbf{R}_{\alpha}) = \int d\mathbf{r}_{\alpha} \phi_{\alpha n}(r_{\alpha}) \mathbf{Z}_{\alpha}(\mathbf{R}_{\alpha}, r_{\alpha}) \phi_{\alpha l}(r_{\alpha}) \quad (17)$$

and if  $\alpha \neq \gamma$ ,  $\mathbf{Z}_{\gamma l}^{\alpha n}$  is the exchange interaction, whose kernel is given by

$$\begin{aligned} \mathbf{Z}_{\gamma l}^{\alpha n}(\mathbf{R}_{\alpha}, \mathbf{R}_{\gamma}) &= - \left( \frac{\partial r_{\alpha}}{\partial \mathbf{R}_{\gamma}} \right)_{\mathbf{R}_{\alpha}} \phi_{\alpha n}(r_{\alpha}) [\kappa_{\gamma l}^2 - T_{\gamma} \\ &\quad - \mathbf{Z}_{\gamma}(\mathbf{R}_{\gamma}, r_{\gamma})] \phi_{\gamma l}(r_{\gamma}), \end{aligned} \quad (18)$$

where  $\kappa_{\gamma l}^2 = 2\mu(E_{\text{ref}} - \epsilon_{\gamma l})/\hbar^2$ , and the Jacobian factor  $(\partial r_{\alpha}/\partial \mathbf{R}_{\gamma})_{\mathbf{R}_{\alpha}}$  results from the transformations  $r_{\alpha} \rightarrow r_{\alpha}(\mathbf{R}_{\alpha}, \mathbf{R}_{\gamma})$  and  $r_{\gamma} \rightarrow r_{\gamma}(\mathbf{R}_{\alpha}, \mathbf{R}_{\gamma})$  for each value of  $\mathbf{R}_{\alpha}$ .

The Y-NVP functional for the  $Y$  matrix element  $Y_{\alpha n, \beta m}$  can now be written as

$$\begin{aligned} Y_{\alpha n, \beta m} &= Y_{\alpha n, \beta m}^0 + \sum_{\gamma l} \{ \langle f_{\alpha n}^0 | \mathbf{Z}_{\gamma l}^{\alpha n} \mathbf{G}_{\gamma l}^0 | f_{\beta m}^{\gamma l} \rangle \\ &\quad + \langle F_{\gamma l}^{\alpha n} | \mathbf{G}_{\gamma l}^0 \mathbf{Z}_{\beta m}^{\gamma l} | f_{\beta m}^0 \rangle - \langle F_{\gamma l}^{\alpha n} | \mathbf{G}_{\gamma l}^0 | F_{\beta m}^{\gamma l} \rangle \} \\ &\quad + \sum_{\gamma l} \sum_{\gamma' l'} \langle F_{\gamma l}^{\alpha n} | \mathbf{G}_{\gamma l}^0 \mathbf{Z}_{\gamma' l'}^{\gamma l} \mathbf{G}_{\gamma' l'}^0 | F_{\beta m}^{\gamma' l'} \rangle, \end{aligned} \quad (19)$$

where

$$Y_{\alpha n, \beta m}^0 = \delta_{\alpha\beta} \delta_{nm} \left( \frac{\partial f_{\alpha n}^0}{\partial \mathbf{R}_{\alpha}} \right)_{\mathbf{R}_{\alpha}} + \langle f_{\alpha n}^0 | \mathbf{Z}_{\beta m}^{\alpha n} | f_{\beta m}^0 \rangle. \quad (20)$$

We expand the amplitude densities in a set of  $L^2$  basis functions  $\{v_i\}_1^N$

$$F_{\gamma l}^{\alpha n}(\mathbf{R}_{\alpha}) = \sum_{i=1}^N |v_i\rangle \langle v_i | F_{\gamma l}^{\alpha n} \rangle. \quad (21)$$

We require the functions with  $i < N$  to satisfy the (0,0) boundary conditions, while the function  $|v_N\rangle$  satisfies the (0,1) conditions. The reason for this choice of functions for the basis is that unlike the GNVP amplitude densities, the Y-NVP amplitude densities do not vanish asymptotically. (See Sec. II D, below.) Substituting the expansion of Eq. (21) into the functional of Eq. (19) and extremizing the functional with respect to the expansion coefficients  $\langle v_i | F_{\gamma l}^{\alpha n} \rangle$ , we arrive at the relationship

$$Y_{\alpha n, \beta m} = Y_{\alpha n, \beta m}^0 + (\mathbf{B}^T \mathbf{A}^{-1} \mathbf{B})_{\alpha n, \beta m}, \quad (22)$$

where

$$\mathbf{B}_{\alpha n, \beta m} = \langle v_i | \mathbf{G}_{\alpha n}^0 \mathbf{Z}_{\beta m}^{\alpha n} | f_{\beta m}^0 \rangle \quad (23)$$

and

$$\begin{aligned} \mathbf{A}_{\alpha n, \beta m j} &= \langle v_i | \mathbf{G}_{\alpha n}^0 | v_j \rangle \delta_{\alpha\beta} \delta_{nm} \\ &\quad - \langle v_i | \mathbf{G}_{\alpha n}^0 \mathbf{Z}_{\beta m}^{\alpha n} \mathbf{G}_{\beta m}^0 | v_j \rangle. \end{aligned} \quad (24)$$

To arrive at the final “working equations” of the log-derivative Newton method, we now recognize the following. Substituting Eq. (15) into Eqs. (17) and (18), we see that

$$\begin{aligned} \mathbf{Z}_{\beta m}^{\alpha n} &= (\mathbf{U}_{\beta m}^{\alpha n} - \lambda_{\beta m} \delta_{nm}) \delta_{\alpha\beta} \\ &\quad + (1 - \delta_{\alpha\beta}) \{ \mathbf{S}_{\beta m}^{\alpha n} (\kappa_{\beta m}^2 - T_{\beta}) + \lambda_{\beta m} \} - \mathbf{U}_{\beta m}^{\alpha n}, \end{aligned} \quad (25)$$

where

$$\mathbf{S}_{\beta m}^{\alpha n} = - \left( \frac{\partial r_{\alpha}}{\partial \mathbf{R}_{\beta}} \right)_{\mathbf{R}_{\alpha}} \phi_{\alpha n}(r_{\alpha}) \phi_{\beta m}(r_{\beta}) \quad (26)$$

and the definitions of  $\mathbf{U}_{\beta m}^{\alpha n}$  and  $\lambda_{\beta m}$  follow from Eqs. (15), (17), and (18). We also recognize that the kinetic energy operator in the second term of Eq. (25) does not appear in our calculations since

$$\begin{aligned} \mathbf{Z}_{\beta m}^{\alpha n} \mathbf{G}_{\beta m}^0 &= (\mathbf{U}_{\beta m}^{\alpha n} - \lambda_{\beta m} \delta_{nm}) \delta_{\alpha\beta} \mathbf{G}_{\beta m}^0 \\ &\quad + (1 - \delta_{\alpha\beta}) \{ \mathbf{S}_{\beta m}^{\alpha n} (1 + \lambda_{\beta m} \mathbf{G}_{\beta m}^0) \\ &\quad - \mathbf{U}_{\beta m}^{\alpha n} \mathbf{G}_{\beta m}^0 \} \end{aligned} \quad (27)$$

and

$$\begin{aligned} \mathbf{Z}_{\beta m}^{\alpha n} f_{\beta m}^0 &= (\mathbf{U}_{\beta m}^{\alpha n} - \lambda_{\beta m} \delta_{nm}) \delta_{\alpha\beta} f_{\beta m}^0 \\ &\quad - (1 - \delta_{\alpha\beta}) \mathbf{U}_{\beta m}^{\alpha n} f_{\beta m}^0. \end{aligned} \quad (28)$$

Splitting matrices  $\mathbf{Y}^0$ ,  $\mathbf{A}$  and  $\mathbf{B}$  in Eq. (22) into “direct” and “exchange” parts, and using Eqs. (25), (27), and (28), we get the direct terms

$$\begin{aligned} (\mathbf{Y}_d^0)_{\alpha n, \beta m} &= \delta_{\alpha\beta} \delta_{nm} \left( \frac{\partial f_{\alpha n}^0}{\partial \mathbf{R}_{\alpha}} \right)_{\mathbf{R}_{\alpha}} + \delta_{\alpha\beta} \langle f_{\alpha n}^0 | \mathbf{U}_{\beta m}^{\alpha n} | f_{\beta m}^0 \rangle \\ &\quad - \delta_{nm} \langle f_{\alpha n}^0 | f_{\beta m}^0 \rangle \lambda_{\beta m}, \end{aligned} \quad (29)$$

$$\begin{aligned} (\mathbf{B}_d)_{\alpha n, \beta m} &= \delta_{\alpha\beta} \langle v_i | \mathbf{G}_{\alpha n}^0 \mathbf{U}_{\beta m}^{\alpha n} | f_{\beta m}^0 \rangle \\ &\quad - \delta_{nm} \langle v_i | \mathbf{G}_{\alpha n}^0 | f_{\beta m}^0 \rangle \lambda_{\beta m}, \end{aligned} \quad (30)$$

$$\begin{aligned} (\mathbf{A}_d)_{\alpha n, \beta m j} &= \langle v_i | \mathbf{G}_{\alpha n}^0 | v_j \rangle \delta_{\alpha\beta} \delta_{nm} \\ &\quad - \delta_{\alpha\beta} \langle v_i | \mathbf{G}_{\alpha n}^0 \mathbf{U}_{\beta m}^{\alpha n} \mathbf{G}_{\beta m}^0 | v_j \rangle \\ &\quad + \delta_{\alpha\beta} (\delta_{nm} \langle v_i | \mathbf{G}_{\alpha n}^0 \mathbf{G}_{\beta m}^0 | v_j \rangle \lambda_{\beta m}), \end{aligned} \quad (31)$$

and the exchange terms

$$\begin{aligned} (\mathbf{Y}_e^0)_{\alpha n, \beta m} &= (1 - \delta_{\alpha\beta}) \langle f_{\alpha n}^0 | \mathbf{U}_{\beta m}^{\alpha n} | f_{\beta m}^0 \rangle \\ &\quad - \langle f_{\alpha n}^0 | \mathbf{S}_{\beta m}^{\alpha n} | f_{\beta m}^0 \rangle \lambda_{\beta m}, \end{aligned} \quad (32)$$

$$\begin{aligned} (\mathbf{B}_e)_{\alpha n, \beta m} &= (1 - \delta_{\alpha\beta}) \langle v_i | \mathbf{G}_{\alpha n}^0 \mathbf{U}_{\beta m}^{\alpha n} | f_{\beta m}^0 \rangle \\ &\quad - \langle v_i | \mathbf{G}_{\alpha n}^0 \mathbf{S}_{\beta m}^{\alpha n} | f_{\beta m}^0 \rangle \lambda_{\beta m}, \end{aligned} \quad (33)$$

$$\begin{aligned} (\mathbf{A}_e)_{\alpha n, \beta m j} &= (1 - \delta_{\alpha\beta}) \langle v_i | \mathbf{G}_{\alpha n}^0 \mathbf{S}_{\beta m}^{\alpha n} | v_j \rangle \\ &\quad - \langle v_i | \mathbf{G}_{\alpha n}^0 \mathbf{U}_{\beta m}^{\alpha n} \mathbf{G}_{\beta m}^0 | v_j \rangle \\ &\quad + (1 - \delta_{\alpha\beta}) \langle v_i | \mathbf{G}_{\alpha n}^0 \mathbf{S}_{\beta m}^{\alpha n} \mathbf{G}_{\beta m}^0 | v_j \rangle \lambda_{\beta m}. \end{aligned} \quad (34)$$

Equations (29)–(34) completely define the quantities that enter the extremized functional of Eq. (22) and are the equations used for the calculations reported in Sec. III. One important property of these equations is that since the scattering energy enters the functional only through the quantities

$$\lambda_{\beta m} = (k_{\beta m}^2 - \kappa_{\beta m}^2) = 2\mu(E - E_{\text{ref}})/\hbar^2, \quad (35)$$

the matrix elements of the Y-NVP functional are *completely independent of the scattering energy and need be evaluated only once*.

### C. Channel independent reference energy Green's functions

The reference problem for the REGFs can be made independent of the asymptotic channel energies by simply removing the Hamiltonian for the internal degrees of freedom from the reference problem. This leads to a REGF of the type<sup>33</sup>

$$\langle \phi_{an} | G_{\alpha}^0 | \phi_{am} \rangle = \delta_{nm} \sum_{ij} |u_i\rangle \langle u_i | \kappa^2 - T_{\alpha} | u_j \rangle^{-1} \langle u_j |, \quad (36)$$

so that the matrix to be inverted is independent of the internal channels. Therefore the matrix inversion needs to be performed only once, *regardless of the number of channels used in the problem*. This is a great advantage when three-dimensional scattering calculations are to be done, since the number of rovibrational channels are usually very large for such problems. However, it is clear that this approach imposes certain restrictions on the type of distortion potentials that may be included in the reference problem. A distortion potential that couples the internal channels would render these REGFs once again channel dependent.

Note that the quantities  $\lambda_{an}$  of Eq. (35) are actually independent of the internal channel, since the internal energy cancels in the difference  $k_{an}^2 - \kappa_{an}^2$ . On the other hand, when the channel independent REGFs are defined as in Eq. (36), the quantities  $\lambda_{an}$  become explicitly channel dependent, as

$$\lambda_{an} = k_{an}^2 - \kappa^2 = 2\mu[(E - \epsilon_{an}) - E_{\text{ref}}]/\hbar^2. \quad (37)$$

### D. The $L^2$ Basis for the Y-NVP amplitude densities

As mentioned in Sec. I, the present *numerical* implementation of the Y-NVP differs from the previous one in that a function  $|\nu_N\rangle$ , which satisfies the (0,1) boundary conditions is now added to the  $L^2$  basis used to expand the amplitude densities. It is instructive to briefly discuss the reasons for the inclusion of this function, and the implications this has for some of the results reported in Ref. 21, where a basis that did not contain such a function was used. Consider a one-dimensional potential scattering case, for example. In contrast to the GNVP amplitude density, the Y-NVP amplitude density  $F(R)$  does not vanish as  $R \rightarrow R_{\text{max}}$  [where  $R_{\text{max}}$  is large enough that  $U(R_{\text{max}}) \approx 0$ ], since

$$\lim_{R \rightarrow a} F(R) = \lim_{R \rightarrow a} [U(R) - \lambda] f(R) = -\lambda, \quad (38)$$

since  $f(a) = 1$ . Therefore, the amplitude density does not vanish asymptotically except when  $\lambda = 0$ , i.e.,  $E = E_{\text{ref}}$ . By including the function  $|\nu_N\rangle$  in the basis, we ensure that the proper boundary conditions can be satisfied. Note that formally, since the functions  $|\nu_i\rangle$ ;  $i < N$  vanish at the boundary  $R = a$ , the expansion coefficient of  $|\nu_N\rangle$  is identically equal to  $-\lambda$ . Then, the system of linear algebraic equations for

the expansion coefficients may be rewritten by pulling all terms containing  $|\nu_N\rangle$  to the right-hand side [similar to our procedure in Eq. (7)]. However, in the present work, we have not done so. The present implementation of the Y-NVP treats all expansion coefficients on an equal footing.

This raises certain questions concerning the numerical results reported in Ref. 21, for cases where  $E \neq E_{\text{ref}}$ . In that work, the basis used to expand the amplitude density did not contain the function  $|\nu_N\rangle$ . Therefore, the basis satisfied the (0,0) boundary conditions even when the amplitude densities did not. In spite of this, however, the calculations using the basis converged rapidly to the correct values. The reason for this can be found in the mathematical relationship between the Kohn and Newton variational methods. As shown in Appendix A, the Kohn functional for the log-derivative  $Y(a)$  can be written in the form

$$I(f_n, f_m) = \left( \frac{df_m}{dr} \right)_{r=a} + (2\mu/\hbar^2) \langle f_n | H - E | f_m \rangle, \quad (39)$$

where  $f_n$  and  $f_m$  are two trial functions that satisfy the (0,1) boundary conditions. Provided that the Lippmann-Schwinger equation is used as a basis for generating successive orders of approximation  $f_n, f_{n+1}$  etc., for a trial function  $f$ , Appendix A shows that the functional  $I(f_0, f_0)$  is the Kohn variational principle, the functional  $I(f_0, f_1)$  is the Schwinger principle, and the functional  $I(f_1, f_1)$  is the Newton variational principle. In each case,  $f_0$  is expanded in an appropriate  $L^2$  basis set  $\{v_i\}_{i=1}^N$  that satisfies the (0,1) boundary conditions. The reason for the convergence of calculations for which  $\lambda \neq 0$  in Ref. 21, in the absence of the function  $|\nu_N\rangle$ , is due to the fact that the function  $f_1$  satisfies the (0,1) boundary conditions, *regardless of the nature* of the basis used to expand  $f_0$ . This can be easily verified by examining the boundary conditions satisfied by Eq. (A5) of Appendix A for arbitrary choices of  $f_0$ . However, for arbitrary choices of  $f_0$ , the Kohn functional  $I(f_0, f_0)$  does not yield a  $Y$  matrix, since the correct boundary conditions are not satisfied. The functional  $I(f_1, f_1)$ , on the other hand, converges at the same rate as a Kohn calculation where  $f_0$  is expanded in a basis that satisfies the (0,1) boundary conditions:

$$f_0 = f_r^0 + \sum_{i=1}^{N-1} G^0[U - \lambda] |\nu_i\rangle. \quad (40)$$

In this sense, the calculations of Ref. 21 for which  $E \neq E_{\text{ref}}$  are actually Kohn calculations using a *reference energy dependent* basis. The functional  $I(f_1, f_1)$  with the expansion of Eq. (40) for  $f_0$  rigorously becomes the Y-NVP functional only when  $\lambda = 0$ , or  $E = E_{\text{ref}}$ . On the other hand, the inclusion of the function  $|\nu_N\rangle$  ensures that the proper relationship between the Kohn and the Newton functionals are maintained at all values of  $E$ .

## III. CALCULATIONS AND RESULTS

In this section, we briefly outline the details of the calculations performed on the collinear H + H<sub>2</sub> system on the PK2 potential surface, and present the results. In what follows, all distances are in Bohr, and all energies in eV. The asymptotic problem for the diatomic vibrational energies

$\epsilon_{\alpha n}$  is solved at  $R_{\max} = 10$ , using a 40 point Lobatto DVR in the interval  $(r_{\min}, r_{\max}) = (0.50, 4.0)$ . This is sufficient to converge the  $\epsilon_{\alpha n}$  of the lowest seven states to five or six significant figures. The reference problem for the REGFs is solved in the domain  $(R_{\min}, R_{\max}) = (1.0, 10.0)$  using a Lobatto DVR of 101 points, as described in Sec. II A. The lower and upper limits of the integrations in the  $r$  and  $R$  coordinates used here are comparable to the values used by previous workers. The 101 point DVR used for the reference problem also defines the quadrature rule for evaluating all the matrix elements of the functional.

The basis set used to expand the projected amplitude densities  $F_{\nu l}^{\alpha n}$  consists of a set of 1- $d$  box energy eigenfunctions

$$|v_j\rangle = \left(\frac{2}{a}\right)^{1/2} \sin\left[\frac{j\pi(R - R_{\min})}{a}\right]; \quad j = 1, \dots, N-1, \quad (41)$$

where  $a = (R_{\max} - R_{\min})$ , and

$$|v_N\rangle = \sinh[\alpha(R - R_{\min})]/\sinh(\alpha a), \quad (42)$$

or

$$|v_N\rangle = (R - R_{\min})/a. \quad (43)$$

Both choices of  $|v_N\rangle$  satisfy the (0,1) boundary conditions. The function of Eq. (42) behaves like a damping function, and is actually the regular solution for the reference problem corresponding to a reference energy of  $-\hbar^2\alpha^2/2\mu$ . Except for very small ( $\leq 0.10$ ) values of the parameter  $\alpha$ , the function of Eq. (42) remains small for  $R \ll R_{\max}$ , and gradually approaches unity as  $R \rightarrow R_{\max}$ . The parameter  $\alpha$  thus determines the range of  $R \approx R_{\max}$  over which the function  $|v_N\rangle$  assumes appreciable values; smaller the value of  $\alpha$ , the larger the range. The function of Eq. (43) is of course, a straight line, or a "ramp" function. We shall see below that the convergence characteristics of the Y-NVP functional is remarkably insensitive to the choice of  $\alpha$  or even the type of function chosen to represent  $|v_N\rangle$ . Unless otherwise specified, we take  $|v_N\rangle$  to be the function of Eq. (42), with  $\alpha = 3$ .

We calculate the reactive transition probabilities  $P_{00}^{\alpha\beta}(E)$  at several energies in the range  $0.40 \leq E \leq 1.65$ . Many previous investigations of the collinear  $H + H_2$  system have examined this energy range. The majority of our calculations have been at scattering energies previously studied by Dardi, Shi, and Miller (DSM).<sup>26</sup>

We first discuss the calculations performed using the channel dependent REGFs. To test the convergence of the  $P_{00}^{\alpha\beta}(E)$  with respect to the number of closed channels included in the calculations, we set  $N$ , the number of  $L^2$  basis functions per channel, to 40 and perform calculations using 4, 5, 6 and 7 channels. The value of  $E_{\text{ref}}$  in these calculations are chosen to be 1.00 eV, which approximately corresponds to the middle of the energy range examined. The results are summarized in Table I. As expected, the lower energy results converge with as few as four channels while the highest energies require up to six channels. The remainder of our calculations are done with six channels at all energies.

The convergence of the Y-NVP with respect to the number of  $L^2$  functions per channel is investigated next, in Table II. Compared to the fully converged  $P_{00}^{\alpha\beta}$ s of Table I, we see that the reactive transition probabilities are converged to

TABLE I. Convergence of the Y-NVP ( $\nu = 0 \rightarrow \nu' = 0$ ) reaction probabilities in the range  $0.40 \leq E \leq 1.65$  eV, with respect to the number of vibrational channels.  $N = 40$ ;  $E_{\text{ref}} = 1.00$  eV.

$E$ (eV)	Number of vibrational channels			
	4	5	6	7
0.4028	2.50(-3)	2.50(-3)	2.50(-3)	2.50(-3)
0.4334	2.65(-2)	2.65(-2)	2.65(-2)	2.65(-2)
0.4546	1.01(-1)	1.01(-1)	1.01(-1)	1.01(-1)
0.4826	3.70(-1)	3.70(-1)	3.70(-1)	3.70(-1)
0.5000	6.01(-1)	6.01(-1)	6.01(-1)	6.01(-1)
0.5376	9.13(-1)	9.13(-1)	9.14(-1)	9.14(-1)
0.6000	9.99(-1)	9.99(-1)	9.99(-1)	9.99(-1)
0.7000	9.91(-1)	9.91(-1)	9.91(-1)	9.91(-1)
0.8000 <sup>a</sup>	9.50(-1)	9.50(-1)	9.50(-1)	9.50(-1)
0.8706	1.84(-1)	1.82(-1)	1.82(-1)	1.82(-1)
0.8976	6.64(-1)	6.66(-1)	6.66(-1)	6.66(-1)
1.0000	5.96(-1)	5.95(-1)	5.95(-1)	5.95(-1)
1.2026	2.27(-1)	2.28(-1)	2.28(-1)	2.28(-1)
1.3000 <sup>b</sup>	5.60(-1)	6.28(-1)	6.30(-1)	6.30(-1)
1.3966	1.26(-1)	1.30(-1)	1.30(-1)	1.30(-1)
1.6466	8.71(-2)	7.55(-2)	7.42(-2)	7.42(-2)

<sup>a</sup> The  $\nu' = 1$  channel becomes open.

<sup>b</sup> The  $\nu' = 2$  channel becomes open.

within 1% or better with about 25 functions per channel for  $E \leq 1.00$  eV. The higher energies require up to 35 functions to reach the same level of convergence. Recall that when the channel dependent REGFs are used, as in Tables I and II, the Y-NVP converges at the same rate as the GNVP for  $E = E_{\text{ref}}$ .<sup>21</sup> This means that the GNVP would converge this problem to within 1% error with approximately 25 functions at  $E = 1.00$  eV. Using the Y-NVP, however, we are able to converge the results for all  $E \leq 1.00$  eV, with *no additional effort* for matrix element evaluations.

We now examine the results of using the channel independent REGFs. Calculations analogous to those of Table II, using the channel independent REGFs are presented in Table III. It is interesting that  $P_{00}^{\alpha\beta}(1.00)$  is better converged with  $N = 25$  here than in Table II. However, with the exception of  $E = 0.60$ , this approach requires  $N = 30$  before the other  $P_{00}^{\alpha\beta}(E)$ s converge to within 1%. Another interesting point to note is that the channel independent REGFs appear to be more efficient at converging the results slightly above  $E_{\text{ref}}$ . The probabilities  $P_{00}^{\alpha\beta}(E)$  in the range  $1.2026 \leq E \leq 1.3966$  are better converged with  $N = 30$  in Table III than in Table II. Considering the significant savings promised by this approach (see Sec. IV), we believe that the Y-NVP calculations using channel independent REGFs offer a very attractive alternative to using the Kohn methods, which generally converge slower.

We now examine two more issues associated with the present approach, viz., the dependence of the  $P_{00}^{\alpha\beta}(E)$ s for a fixed value of  $N$  on (a)  $E_{\text{ref}}$ , and (b) the nature of the function  $|v_N\rangle$  used in the  $L^2$  basis. Table IV addresses the first issue, by calculating  $P_{00}^{\alpha\beta}(E)$ s for several energies in the range  $0.40 \leq E \leq 1.65$ , with  $N = 30$ , for five values of  $E_{\text{ref}}$ . This Table indicates that for  $E_{\text{ref}} = 0.0, 0.50$ , and 1.00, the method achieves fairly similar levels of accuracy with

TABLE II. Convergence of the Y-NVP ( $\nu = 0 \rightarrow \nu' = 0$ ) reaction probabilities in the range  $0.40 \leq E \leq 1.65$  eV, when channel dependent REGFs are used. A total of six channels are used in these calculations.  $E_{\text{ref}} = 1.00$  eV.

$E$ (eV)	Number of $L^2$ functions					
	15	20	25	30	35	40
0.4028	2.75(-3)	2.61(-3)	2.51(-3)	2.51(-3)	2.50(-3)	2.50(-3)
0.4334	3.66(-2)	2.98(-2)	2.67(-2)	2.65(-2)	2.65(-2)	2.65(-2)
0.4546	7.06(-2)	9.24(-2)	1.00(-1)	1.01(-1)	1.01(-1)	1.01(-1)
0.4826	2.24(-1)	3.13(-1)	3.66(-1)	3.69(-1)	3.70(-1)	3.70(-1)
0.5000	8.09(-1)	6.80(-1)	6.05(-1)	6.02(-1)	6.01(-1)	6.01(-1)
0.5376	9.85(-1)	9.51(-1)	9.16(-1)	9.14(-1)	9.14(-1)	9.14(-1)
0.6000	3.01(-1)	1.00	9.99(-1)	9.99(-1)	9.99(-1)	9.99(-1)
0.7000	5.55(-3)	8.68(-1)	9.90(-1)	9.90(-1)	9.91(-1)	9.91(-1)
0.8000 <sup>a</sup>	4.23(-1)	9.99(-1)	9.51(-1)	9.50(-1)	9.50(-1)	9.50(-1)
0.8706	3.55(-2)	2.15(-1)	1.83(-1)	1.82(-1)	1.82(-1)	1.82(-1)
0.8976	9.26(-4)	5.31(-2)	6.67(-1)	6.66(-1)	6.66(-1)	6.66(-1)
1.0000	3.38(-4)	7.99(-2)	6.00(-1)	5.95(-1)	5.95(-1)	5.95(-1)
1.2026	6.13(-3)	1.73(-2)	1.39(-1)	2.29(-1)	2.28(-1)	2.28(-1)
1.3000 <sup>b</sup>	1.16(-3)	3.87(-2)	4.05(-1)	6.31(-1)	6.30(-1)	6.30(-1)
1.3966	4.78(-3)	4.86(-2)	2.12(-2)	1.37(-1)	1.30(-1)	1.30(-1)
1.6466	1.56(-1)	1.10(-2)	2.82(-2)	6.76(-2)	7.38(-2)	7.42(-2)

<sup>a</sup>The  $\nu' = 1$  channel becomes open.

<sup>b</sup>The  $\nu' = 2$  channel becomes open.

$N = 30$ , except at the two highest energies examined. However, the convergence at all energies are very poor when  $E_{\text{ref}} = 1.65$ . A tentative explanation for this rather puzzling behavior is as follows. Note that when  $E_{\text{ref}} > 0$ , the channel independent REGFs resemble the open channel Green's functions of Fig. 1 (a). The larger the value of  $E_{\text{ref}}$ , the more oscillatory this function becomes. When such highly oscillatory functions are present in the functional, the basis functions have to be sufficiently oscillatory as well, in order to cancel out the unwanted oscillations in the Green's func-

tions. Apparently, the sine functions  $|\nu_i\rangle$ , with  $i \leq 29$  are not able to fulfill this role. In support of this explanation, we also present, in Table IV, the results of performing these calculations with  $E_{\text{ref}} = -1.65$ . The negative value of  $E_{\text{ref}}$  yields a nonoscillatory, closed channel REGF of the type shown in Fig. 1 (b). It is clear that the results using such a Green's function are much better converged than those using the highly oscillatory REGF that results from a large, positive  $E_{\text{ref}}$ .

The second issue raised above is potentially more impor-

TABLE III. Convergence of the Y-NVP ( $\nu = 0 \rightarrow \nu' = 0$ ) reaction probabilities in the range  $0.40 \leq E \leq 1.65$  eV, when channel independent REGFs are used. A total of six channels are used in these calculations.  $E_{\text{ref}} = 1.00$  eV.

$E$ (eV)	Number of $L^2$ functions				
	20	25	30	35	40
0.4028	2.62(-3)	2.55(-3)	2.51(-3)	2.50(-3)	2.50(-3)
0.4334	2.99(-2)	2.78(-2)	2.66(-2)	2.65(-2)	2.65(-2)
0.4546	9.28(-2)	9.49(-2)	1.00(-1)	1.01(-1)	1.01(-1)
0.4826	3.11(-1)	3.39(-1)	3.68(-1)	3.69(-1)	3.70(-1)
0.5000	6.81(-1)	6.36(-1)	6.03(-1)	6.02(-1)	6.01(-1)
0.5376	9.53(-1)	9.32(-1)	9.15(-1)	9.14(-1)	9.14(-1)
0.6000	1.00	1.00	9.99(-1)	9.99(-1)	9.99(-1)
0.7000	8.63(-1)	9.62(-1)	9.90(-1)	9.90(-1)	9.91(-1)
0.8000 <sup>a</sup>	9.99(-1)	9.70(-1)	9.51(-1)	9.50(-1)	9.50(-1)
0.8706	1.98(-1)	1.41(-1)	1.81(-1)	1.82(-1)	1.82(-1)
0.8976	3.86(-2)	6.86(-1)	6.66(-1)	6.66(-1)	6.66(-1)
1.0000	2.96(-1)	5.93(-1)	5.95(-1)	5.95(-1)	5.95(-1)
1.2026	6.84(-4)	4.13(-2)	2.28(-1)	2.28(-1)	2.28(-1)
1.3000 <sup>b</sup>	1.06(-1)	6.94(-1)	6.30(-1)	6.30(-1)	6.30(-1)
1.3966	6.44(-2)	1.68(-2)	1.32(-1)	1.30(-1)	1.30(-1)
1.6466	6.85(-3)	3.64(-2)	9.06(-2)	7.40(-2)	7.41(-2)

<sup>a</sup>The  $\nu' = 1$  channel becomes open.

<sup>b</sup>The  $\nu' = 2$  channel becomes open.

TABLE IV. Dependence of the Y-NVP ( $\nu = 0 \rightarrow \nu' = 0$ ) reaction probabilities in the range  $0.40 \leq E \leq 1.65$  eV, on the reference energy. The basis consists of 30  $L^2$  functions in each of six channels. Channel independent REGFs are used.

$E$ (eV)	Reference energy $E_{\text{ref}}$ (eV)				
	0.0	0.5	1.0	1.65	-1.65
0.4028	2.50(-3)	2.50(-3)	2.51(-3)	2.54(-3)	2.51(-3)
0.4334	2.65(-2)	2.65(-2)	2.66(-2)	2.75(-2)	2.66(-2)
0.4546	1.01(-2)	1.01(-2)	1.00(-1)	9.90(-2)	1.01(-1)
0.4826	3.70(-1)	3.70(-1)	3.68(-1)	3.52(-1)	3.67(-1)
0.5000	6.01(-1)	6.01(-1)	6.03(-1)	6.24(-1)	6.03(-1)
0.5376	9.14(-1)	9.14(-1)	9.15(-1)	9.27(-1)	9.14(-1)
0.6000	9.99(-1)	9.99(-1)	9.99(-1)	9.99(-1)	9.99(-1)
0.7000	9.90(-1)	9.91(-1)	9.90(-1)	9.76(-1)	9.90(-1)
0.8000 <sup>a</sup>	9.51(-1)	9.51(-1)	9.51(-1)	9.59(-1)	9.51(-1)
0.8706	1.81(-1)	1.82(-1)	1.81(-1)	1.60(-1)	1.79(-1)
0.8976	6.66(-1)	6.66(-1)	6.66(-1)	6.80(-1)	6.68(-1)
1.0000	5.96(-1)	5.95(-1)	5.95(-1)	6.03(-1)	5.98(-1)
1.2026	2.31(-1)	2.30(-1)	2.28(-1)	2.31(-1)	2.33(-1)
1.3000 <sup>b</sup>	6.33(-1)	6.32(-1)	6.30(-1)	6.20(-1)	6.35(-1)
1.3966	1.45(-1)	1.39(-1)	1.32(-1)	1.93(-1)	1.55(-1)
1.6466	5.12(-2)	6.41(-2)	9.06(-2)	1.97(-2)	3.99(-2)

<sup>a</sup>The  $\nu' = 1$  channel becomes open.

<sup>b</sup>The  $\nu' = 2$  channel becomes open.



tant for the routine application of the Y-NVP to scattering problems. Table V summarizes the results of computing the  $P_{\infty}^{\alpha\beta}(E)$ s with  $N = 30$ , where the damping function of Eq. (43) with several choices of the parameter  $\alpha$  and the ramp function of Eq. (44) have been used for the function  $|\nu_N\rangle$ . The reference energy is chosen to be 0. Table V indicates that the convergence rate of the Y-NVP is remarkably insensitive to the value of the parameter  $\alpha$ , or even to the nature of the function chosen for  $|\nu_N\rangle$ .

Finally, to summarize the results of our calculations and to compare them to those of DSM,<sup>26</sup> we present in Fig. 2, the results of performing the Y-NVP calculations at 32 energies in the range  $0.40 \leq E \leq 1.65$ . For these calculations, channel independent REGFs are used,  $N = 35$  and  $E_{\text{ref}} = 1.00$  eV. The solid line is a smooth curve drawn through the results of these calculations. The results of DSM<sup>26</sup> are plotted as dots. Clearly the agreement is very good at all energies. This figure also illustrates the power of the present method. We are able to generate all the results shown in this figure as the solid line, *with essentially no more effort than a Y-KVP calculation to compute the same results.*

#### IV. DISCUSSION

We have applied the Newton variational method for the log-derivative matrix (the Y-NVP) to the case of the collinear  $\text{H} + \text{H}_2$  reaction on the PK2 surface. An important feature of the Y-NVP is that the matrix elements of the variational functional are independent of the scattering energy, and therefore, need be calculated only once. This feature allows us to perform scattering calculations over a wide range of scattering energies with substantially less computational effort than the GNVP. The energy independence of the Y-NVP matrix elements arise as follows: the log-deriva-

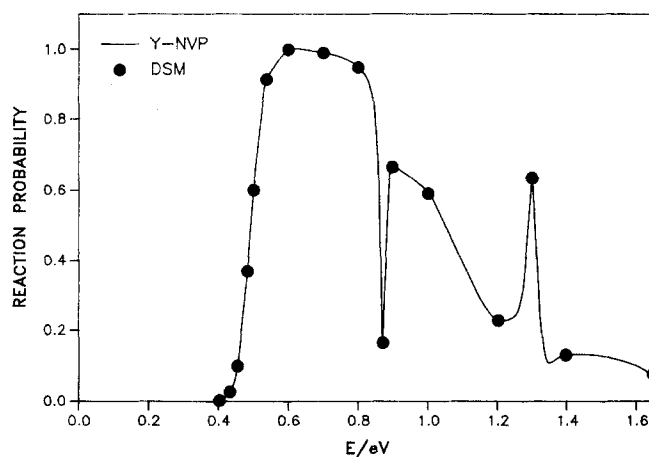


FIG. 2. Reactive transition probabilities  $P_{\infty}^{\alpha\beta}(E)$  for the collinear  $\text{H} + \text{H}_2$  problem on the PK2 surface. The curve passes through the Y-NVP results calculated at 32 energies between 0.40 and 1.65 eV.  $E_{\text{ref}} = 1.00$  eV. The dots are the results of Dardi, Shi, and Miller, taken from Ref. 26.

tive boundary conditions, unlike the  $K$ ,  $S$  or  $T$  matrix boundary conditions, are energy independent. This means that the Green's functions of the Y-NVP functional can be defined with respect to a "reference energy" (a constant). The reference problem for these *reference energy Green's functions* REGFs could be restricted to a purely one-dimensional problem—which would mean that the REGFs are independent of the asymptotic internal channels—or it may be made to contain the Hamiltonian for the internal degrees of freedom—which would result in the channel-dependent REGFs.

The results of the present investigation indicate that the

TABLE V. Dependence of the Y-NVP ( $\nu = 0 \rightarrow \nu' = 0$ ) reaction probabilities in the range  $0.40 \leq E \leq 1.65$  eV, on the basis function that satisfies the (0,1) boundary conditions. The basis consists of  $30 L^2$  functions in each of six channels. Channel independent REGFs are used.  $E_{\text{ref}} = 0.00$  eV.

$E$ (eV)	Value of parameter $\alpha$					
	Ramp	1.0	2.0	3.0	4.0	5.0
0.4028	2.50(-3)	2.50(-3)	2.50(-3)	2.50(-3)	2.50(-3)	2.50(-3)
0.4334	2.65(-2)	2.65(-2)	2.65(-2)	2.65(-2)	2.65(-2)	2.65(-2)
0.4546	1.01(-1)	1.01(-1)	1.01(-1)	1.01(-1)	1.01(-1)	1.01(-1)
0.4826	3.70(-1)	3.70(-1)	3.70(-1)	3.70(-1)	3.70(-1)	3.70(-1)
0.5000	6.01(-1)	6.01(-1)	6.01(-1)	6.01(-1)	6.01(-1)	6.01(-1)
0.5376	9.14(-1)	9.13(-1)	9.14(-1)	9.14(-1)	9.14(-1)	9.14(-1)
0.6000	9.99(-1)	9.99(-1)	9.99(-1)	9.99(-1)	9.99(-1)	9.99(-1)
0.7000	9.90(-1)	9.91(-1)	9.91(-1)	9.90(-1)	9.90(-1)	9.90(-1)
0.8000 <sup>a</sup>	9.51(-1)	9.51(-1)	9.51(-1)	9.51(-1)	9.51(-1)	9.51(-1)
0.8706	1.82(-1)	1.82(-1)	1.82(-1)	1.81(-1)	1.81(-1)	1.81(-1)
0.8976	6.66(-1)	6.66(-1)	6.66(-1)	6.66(-1)	6.66(-1)	6.66(-1)
1.0000	5.96(-1)	5.96(-1)	5.96(-1)	5.96(-1)	5.96(-1)	5.96(-1)
1.2026	2.31(-1)	2.31(-1)	2.31(-1)	2.31(-1)	2.31(-1)	2.31(-1)
1.3000 <sup>b</sup>	6.33(-1)	6.33(-1)	6.33(-1)	6.33(-1)	6.34(-1)	6.34(-1)
1.3966	1.44(-1)	1.44(-1)	1.44(-1)	1.45(-1)	1.46(-1)	1.46(-1)
1.6466	5.26(-1)	5.24(-2)	5.19(-2)	5.12(-2)	5.01(-2)	4.90(-2)

<sup>a</sup> The  $\nu' = 1$  channel becomes open.

<sup>b</sup> The  $\nu' = 2$  channel becomes open.

channel-dependent REGFs offer slightly faster convergence as the number of  $L^2$  functions are increased, while the channel-independent REGFs offer an even further reduction in the computational effort, compared to the GNVP. The convergence tests summarized in Tables II and III show that either approach is capable of achieving rapid convergence over a wide range of energy, even when scattering resonances are encountered. The range of energy over which the REGFs are effective appear to be at least about 1.00 eV, since the method achieves rapid convergence in the range  $0.40 \leq E \leq 1.40$  eV. This is a sizeable range for atom-molecule scattering studies, and is quite sufficient to bring out the details of "interesting" features such as scattering resonances. The possibility remains open that distorted wave Green's functions may be effective over an even larger range of scattering energies.

We have stated that the computational effort involved in implementing the Y-NVP is quite comparable to that of the Y-KVP. The following execution times, on one processor of a Cray X-MP/24, substantiate this claim. Using the channel-dependent REGFs—which means that the Green's functions are found in each channel—in a six-channel calculation, it takes a total of 2.4 s to evaluate the REGFs  $G_{an}^0$  in all six channels. Computation of the direct matrices  $U_{am}^{an}$ , the exchange matrices  $U_{\beta m}^{an}$  and the overlap matrices  $S_{\beta m}^{an}$  take a total of 43 s. It takes another 0.68 s to evaluate all the matrix elements of the Y-NVP functional. The total "overhead" before the linear algebraic problem is solved for the  $Y$ -matrix is, therefore, 46 s. However, 91% of this overhead, i.e., evaluation of the  $U_{am}^{an}$ ,  $U_{\beta m}^{an}$ , and  $S_{\beta m}^{an}$ , are common to both the Y-NVP and the Y-KVP. Therefore, the Y-NVP requires, at the most, only 3 s more than the Y-KVP to calculate the transition probabilities at several energies. Using channel independent REGFs reduces this difference even further, since the evaluation of the Green's functions now take only one-sixth the time reported above, i.e., 0.39 s. This means that 95% of the total overhead is shared by the Y-NVP and the Y-KVP. The actual difference in the time taken for these calculations is almost certainly much less for the following reasons. One, we have not included in the above, the time required to evaluate the matrix elements of the Y-KVP functional. Two, the linear algebraic problem solved in the Y-KVP is often much larger than that in the Y-NVP for the same level of convergence.

We believe that the results presented in Sec. III and the execution times quoted above convincingly demonstrate the usefulness of the Y-NVP. Several aspects concerning the extension of the present method to three dimensional scattering problems are currently under investigation.

## ACKNOWLEDGMENTS

B. R. acknowledges the receipt of a Faculty Development Grant from Louisiana Tech University for the continuation of this work. Generous grants of CPU time on the Cray X-MP/24 and the Cray X-MP/14Se at the University of Texas Center for High Performance Computing are gratefully acknowledged. We also thank the referee for extremely helpful comments. Supported in part by grants from the Na-

tional Science Foundation and the Robert A. Welch Foundation.

## APPENDIX A: THE RELATIONSHIP BETWEEN THE KOHN, SCHWINGER, AND NEWTON VARIATIONAL FUNCTIONALS FOR THE LOG-DERIVATIVE MATRIX

Consider the functional  $\langle \psi | H - E | \psi \rangle$  in the domain  $(0, a)$ , which, with simple manipulations, leads to

$$(2\mu/\hbar^2) \langle \psi | H - E | \psi \rangle = -\psi(d\psi/dr)|_0^a + \int_0^a (d\psi/dr)^2 dr + \int_0^a \psi[U(r) - k^2]\psi dr. \quad (A1)$$

Comparing this to the variational expression for the log-derivative  $Y(a)$ , given by Kohn,<sup>15,29</sup>

$$Y(a) = \int_0^a (d\psi/dr)^2 dr + \int_0^a \psi[U(r) - k^2]\psi dr \quad (A2)$$

we see that an alternate expression for  $Y(a)$  is given by

$$Y(a) = (d\psi/dr)_{r=a} + (2\mu/\hbar^2) \langle \psi | H - E | \psi \rangle, \quad (A3)$$

where the solution  $\psi(r)$  is required to satisfy the (0,1) boundary conditions. We denote the functional of Eq. (A3) as  $I(\psi, \psi)$ . This expression may be further generalized as

$$I(\phi, \psi) = (d\psi/dr)_{r=a} + (2\mu/\hbar^2) \langle \phi | H - E | \psi \rangle, \quad (A4)$$

where both trial functions satisfy the usual (0,1) conditions. The accuracy of the functional of Eq. (A4), of course, depends on how well the trial functions approximate the exact solution. The Lippmann-Schwinger equation provides a systematic way of improving a given trial function  $f_0(r)$ , as in

$$f_1 = f_r^0 + G^0 U f_0, \quad (A5)$$

where  $f_r^0$  is the regular solution to the reference problem  $(H_0 - E)f^0 = 0$  (the irregular solution being denoted as  $f_i^0$ ),  $U = 2\mu V/\hbar^2$ , where  $V = H - H_0$ , and

$$G^0(r, r') = f_r^0(r_<) \Omega^{-1} f_i^0(r_>), \quad (A6)$$

where  $(r_<, r_>)$  are the lesser and greater, respectively, of  $(r, r')$ . The constant  $\Omega$  is given by the Wronskian

$$\Omega = f_r^0(df_i^0/dr) - f_i^0(df_r^0/dr). \quad (A7)$$

Now, from Eq. (A3), we see that  $I(f_0, f_0)$  is the Y-KVP. The functional  $I(f_0, f_1)$  simplifies to

$$I(f_0, f_1) = \left(\frac{df_r^0}{dr}\right)_{r=a} + \langle f_r^0 | U | f_0 \rangle + \langle f_0 | U | f_r^0 \rangle - \langle f_0 | U - UG^0U | f_0 \rangle, \quad (A8)$$

which is the Y-SVP. The following results are used in this simplification:

$$\Omega^{-1}(df_i^0/dr)_{r=a} = 1,$$

$$\left(\frac{df_1}{dr}\right)_{r=a} = \left(\frac{df_r^0}{dr}\right)_{r=a} + \langle f_r^0 | U | f_0 \rangle,$$

$$(H_0 - E)f_r^0 = 0,$$

and

$$(H_0 - E)G^0 = -1.$$

Similarly, it is easy to show that

$$I(f_1, f_1) = \left( \frac{df_r^0}{dr} \right)_{r=a} + \langle f_r^0 | U | f_r^0 \rangle + \langle f_0 | UG^0 U | f_r^0 \rangle \\ + \langle f_r^0 | UG^0 U | f_0 \rangle \\ - \langle f_0 | U(G^0 - G^0 UG^0) U | f_0 \rangle, \quad (\text{A9})$$

which is the Y-NVP for the wave function (as opposed to the amplitude density). Defining the amplitude density as  $F_0 = Uf_0$ , the amplitude density form of the functional is easily obtained. This establishes the explicit mathematical relationships between the Kohn, Schwinger and Newton methods for the log-derivative matrix. Equations (A8) and (A9) also represent somewhat more illuminating derivations of the respective variational methods than the ones presented in Ref. 21. We also note that similar relationships between the Kohn, Schwinger and Newton variational methods for the  $K$  matrix has been derived by Takatsuka *et al.*<sup>34</sup>

## APPENDIX B: ANOMALOUS SINGULARITIES IN THE NEWTON VARIATIONAL FUNCTIONAL FOR THE LOG-DERIVATIVE MATRIX

The presence of spurious singularities have been observed in the Kohn<sup>35</sup> and Schwinger<sup>36</sup> variational methods for the  $K$  matrix. Such singularities usually occur when the matrix  $\mathbf{A}$  of linear system of equations  $\mathbf{AC} = \mathbf{B}$ , becomes singular for some choice of the parameters that characterize the equations. These singularities, of course, have nothing to do with the scattering phenomena the method is supposed to describe.

From the functional (A4) of Appendix A, it is easy to see that the basis of the variational methods for the log-derivative is in finding a solution (once again considering a one-dimensional problem as example)  $f_n(r)$  to the Dirichlet problem

$$(H - E)f_n(r) = 0, \quad 0 \leq r \leq a, \quad (\text{B1})$$

$$f_n(0) = 0, \quad f_n(a) = 1. \quad (\text{B2})$$

A necessary and sufficient condition for the existence of  $f_n(r)$  is that  $E$  not be an eigenvalue of the homogenous problem

$$(H - E)f(r) = 0, \quad 0 \leq r \leq a, \quad (\text{B3})$$

$$f(0) = 0, \quad f(a) = 0. \quad (\text{B4})$$

Therefore, whenever the scattering energy  $E$  becomes identically equal to one of the eigenvalues of the problem in Eq. (B3), the solution  $f_n(r)$  and the log-derivative  $Y(a)$  do not exist. However, as pointed out by Manolopoulos *et al.*,<sup>16</sup> this does not cause any problems in practice. Since the discrete eigenvalues of the problem of Eq. (B3) are of zero measure on the real axis, the chances of choosing a scattering energy that matches an eigenvalue *exactly* is exceedingly small.

In the case of the Y-NVP, we should also be concerned about the existence of the solutions  $f_r^0$  and  $f_i^0$  of the reference problem. The arguments are similar to those above, except that now we are concerned with the reference energy  $E_{\text{ref}}$  being identical to one of the eigenvalues of the homogenous

problem. Once again, this would be a very rare coincidence in actual practice, and can easily be avoided by changing the reference energy by a small amount.

It should be noted that any method that depends on the solution of a real linear system of equations which depend on some parameter, can become unstable for particular choices of the parameter. For example, the S-KVP of Zhang and Miller<sup>14</sup> avoids this problem<sup>37</sup> only in principle. The argument is that in this method, the matrix inverted is complex symmetric rather than real symmetric, as in the other methods discussed above. This means that the matrix cannot become singular for *any* value of the purely real scattering energy. In practice however, the Löwdin-Feshbach partitioning<sup>14</sup> separates out the complex part, and the matrix actually inverted is a real symmetric one that depends parametrically on the (real) scattering energy. However, due to the reasons mentioned above, no difficulties are encountered in practice.<sup>1,2,13,14</sup>

- <sup>1</sup> J. Z. H. Zhang and W. H. Miller, Chem. Phys. Lett. **153**, 465 (1988).
- <sup>2</sup> J. Z. H. Zhang and W. H. Miller, J. Chem. Phys. **91**, 1528 (1989).
- <sup>3</sup> D. E. Manolopoulos and R. E. Wyatt, Chem. Phys. Lett. **159**, 123 (1989); J. Chem. Phys. **92**, 810 (1990).
- <sup>4</sup> M. Mladenovic, M. Zhao, D. G. Truhlar, D. W. Schwenke, Y. Sun, and D. J. Kouri, J. Phys. Chem. **92**, 7035 (1988).
- <sup>5</sup> J. M. Launay and M. Le Dourneuf, Chem. Phys. Lett. **163**, 178 (1989).
- <sup>6</sup> R. T Pack and G. A. Parker, J. Chem. Phys. **87**, 3888 (1987); G. A. Parker, R. T Pack, B. J. Archer, and R. B. Walker, Chem. Phys. Lett. **137**, 564 (1987).
- <sup>7</sup> A. Kuppermann and P. G. Hipes, J. Chem. Phys. **84**, 5962 (1986); P. G. Hipes and A. Kuppermann, Chem. Phys. Lett. **133**, 1 (1987); S. A. Cuccaro, P. G. Hipes, and A. Kuppermann, *ibid.* **154**, 155 (1989); **157**, 440 (1989).
- <sup>8</sup> G. C. Schatz, Chem. Phys. Lett. **150**, 92 (1988).
- <sup>9</sup> M. Baer, J. Chem. Phys. **90**, 3043 (1989).
- <sup>10</sup> F. Webster and J. C. Light, J. Chem. Phys. **85**, 4744 (1986); **90**, 265, 300 (1989).
- <sup>11</sup> J. Lindeberg, S. B. Padjaer, Y. Ohrn, and B. Vessal, J. Chem. Phys. **90**, 6254 (1989).
- <sup>12</sup> W. H. Miller and B. M. D. D. Jansen op de Haar, J. Chem. Phys. **86**, 6213 (1987).
- <sup>13</sup> J. Z. H. Zhang and W. H. Miller, Chem. Phys. Lett. **140**, 329 (1987); J. Chem. Phys. **88**, 4549 (1988).
- <sup>14</sup> J. Z. H. Zhang, S. -I. Chu, and W. H. Miller, J. Chem. Phys. **88**, 6233 (1988).
- <sup>15</sup> D. E. Manolopoulos and R. E. Wyatt, Chem. Phys. Lett. **152**, 23 (1988).
- <sup>16</sup> D. E. Manolopoulos, M. D'Mello, and R. E. Wyatt, J. Chem. Phys. **91**, 6096 (1989).
- <sup>17</sup> D. W. Schwenke, K. Haug, M. Zhao, D. G. Truhlar, Y. Sun, J. Z. H. Zhang, and D. J. Kouri, J. Phys. Chem. **92**, 3202 (1988).
- <sup>18</sup> D. W. Schwenke, K. Haug, D. G. Truhlar, Y. Sun, J. Z. H. Zhang, and D. J. Kouri, J. Phys. Chem. **91**, 6080 (1987).
- <sup>19</sup> M. Zhao, D. G. Truhlar, D. J. Kouri, Y. Sun, and D. W. Schwenke, Chem. Phys. Lett. **156**, 281 (1989); C. Yu, D. J. Kouri, M. Zhao, D. G. Truhlar, and D. W. Schwenke, *ibid.* **157**, 491 (1989); M. Mladenovic, M. Zhao, D. G. Truhlar, D. W. Schwenke, Y. Sun, and D. J. Kouri, *ibid.* **146**, 358 (1988); M. Mladenovic, D. G. Truhlar, D. W. Schwenke, Y. Sun, D. J. Kouri, and N. C. Blais, J. Am. Chem. Soc. **111**, 852 (1989).
- <sup>20</sup> D. W. Schwenke, M. Mladenovic, M. Zhao, D. G. Truhlar, Y. Sun, and D. J. Kouri, in *Supercomputer Algorithms for Reactivity, Dynamics and Kinetics of Small Molecules*, edited by A. Lagana, NATO ASI Series (Kluwer Academic, Dordrecht, 1989).
- <sup>21</sup> B. Ramachandran and R. E. Wyatt, J. Chem. Phys. **91**, 1096 (1989).
- <sup>22</sup> D. Thirumalai and D. G. Truhlar, Chem. Phys. Lett. **70**, 330 (1980).
- <sup>23</sup> B. Ramachandran, T. -G. Wei, and R. E. Wyatt, J. Chem. Phys. **89**, 6785 (1988).

- <sup>24</sup>B. Ramachandran, T. -G. Wei, and R. E. Wyatt, *Chem. Phys. Lett.* **151**, 540 (1988).
- <sup>25</sup>R. N. Porter and M. Karplus, *J. Chem. Phys.* **40**, 1105 (1964).
- <sup>26</sup>P. S. Dardi, S. Shi, and W. H. Miller, *J. Chem. Phys.* **83**, 575 (1985).
- <sup>27</sup>For example, R. I. Altkorn and G. C. Schatz, *J. Chem. Phys.* **72**, 3337 (1980); J. W. Duff and D. G. Truhlar, *Chem. Phys. Lett.* **23**, 327 (1973); S. Wu, B. R. Johnson, and R. D. Levine, *Mol. Phys.* **25**, 609 (1973); J. C. Light and R. B. Walker, *J. Chem. Phys.* **65**, 4272 (1976).
- <sup>28</sup>W. H. Miller, *J. Chem. Phys.* **50**, 407 (1969).
- <sup>29</sup>W. Kohn, *Phys. Rev.* **74**, 1763 (1948).
- <sup>30</sup>For example, see G. Arfken, *Mathematical Methods for Physicists* (Academic, Orlando, FL, 1985), Chap. 16; G. F. Roach, *Green's Functions*, 2nd ed. (Cambridge University, Cambridge, 1970), p. 4.
- <sup>31</sup>Many iterative methods based on the Lanczos or the Block Lanczos algorithms have been used to find resolvents of matrices. For example, C. Duneczky and R. E. Wyatt, *J. Chem. Phys.* **87**, 4519 (1987); M. D'Mello, C. Duneczky, and R. E. Wyatt, *Chem. Phys. Lett.* **148**, 169 (1988); C. M. M. Nex, in *Practical Iterative Methods for Large Scale Computations*, edited by D. L. Boley, D. G. Truhlar, Y. Saad, R. E. Wyatt, and L. A. Collins (North-Holland, Amsterdam, 1989), p. 141.
- <sup>32</sup>Meaning that the reduced mass is the same in all arrangements. See, e.g., J. Z. H. Zhang, D. J. Kouri, K. Haug, D. W. Schwenke, Y. Shima, and D. G. Truhlar, *J. Chem. Phys.* **88**, 2492 (1988). The term "isoinertial" was suggested to us by Professor D. G. Truhlar.
- <sup>33</sup>See the comments on the notation just below Eq. (5).
- <sup>34</sup>K. Takatsuka, R. Lucheese, and V. McKoy, *Phys. Rev. A* **24**, 1812 (1981).
- <sup>35</sup>R. K. Nesbet, *Variational Methods in Atom-Electron Scattering Theory* (Plenum, New York, 1980), Sec. 2.3; C. Schwartz, *Phys. Rev.* **124**, 1468 (1961); *Ann. Phys. (New York)* **10**, 36 (1961).
- <sup>36</sup>B. Apagyi, P. Levay, and K. Ladanyi, *Phys. Rev. A* **37**, 4577 (1988).
- <sup>37</sup>L. F. X. Gaucher and W. H. Miller, *Isr. J. Chem.* **29**, 349 (1989).